Results in Physics 6 (2016) 817–823

Contents lists available at ScienceDirect

Results in Physics

journal homepage: www.journals.elsevier.com/results-in-physics

MHD flow of Jeffrey liquid due to a nonlinear radially stretched sheet in presence of Newtonian heating

T. Hayat [a,b], Gulnaz Bashir [a], M. Waqas [a,*], A. Alsaedi [b]

[a] Department of Mathematics, Quaid-I-Azam University 45320, Islamabad 44000, Pakistan
[b] Department of Mathematics, Faculty of Science, King Abdulaziz University, Jeddah 21589, Saudi Arabia

ARTICLE INFO

Article history:
Received 4 September 2016
Received in revised form 21 September 2016
Accepted 1 October 2016
Available online 4 October 2016

Keywords:
MHD
Jeffrey fluid
Nonlinear stretching sheet
Newtonian heating

ABSTRACT

This communication describes the magnetohydrodynamic (MHD) flow of Jeffrey liquid persuaded by a nonlinear radially stretched sheet. Heat transfer is characterized by Newtonian heating and Joule heating effects. The transformed nonlinear governing ordinary differential equations are solved employing homotopic approach. The obtained results of the velocity and temperature are analyzed graphically for various pertinent parameters. Skin friction coefficient and Nusselt number are tabulated and addressed for the various embedded parameters. Furthermore the temperature decays for increasing nonlinear parameter of axisymmetric stretching surface. The nonlinear parameter has reverse effect for temperature and skin friction coefficient.

Introduction

The non-Newtonian materials are now considered more useful than the viscous fluids. It is in view their ample applications in engineering, industry and physiology. However diverse characteristics of all materials in such applications cannot be predicted by one fluid model. Hence several constitutive relationships for non-Newtonian materials have been suggested. Jeffrey fluid is one amongst such materials characterizing the salient features of relaxation and retardation times [1, 2, 3, 4, 5]. It is also well-known reality that stretched flows in presence of heat transfer occur in chemical and manufacturing procedures such as wire drawing, glass blowing, artificial fibers, continual casting of metals, liquid films in moisture, paper production, artificial films etc. Hydromagnetic stretched flow in presence of heat transfer finds application to sheet extrusion in order to make flat plastic sheets. Thus heat transfer and cooling for finishing of end product in such applications seems very important. Having such in mind several researchers in the past studied the flows of viscous and non-Newtonian materials towards linear stretched surface with constant temperature or heat flux. The circumstance where heat is transferred to the convective liquid by means of a bounding surface keeping limited heat capacity is named conjugate convective flows or Newtonian heating. Such pattern arises in convection flows system once the heat is injected through solar radiations. Furthermore the Newtonian heating situation arises in several vital engineering devices including conjugate heat transfer around fins and heat exchanger. Thus in perspective of such applications some researchers have utilized the concept of Newtonian heating boundary condition under different physical aspects. Merkin [6] in his initial work reported the stretched flow of viscous liquid in presence of Newtonian heating. Salleh et al. [7] considered Newtonian heating effects in flow of viscous liquid towards stretched surface. Analysis provided by [7] is extended by Hayat et al. [8] for second grade fluid. Makinde [9] studied the flow of viscous material with Navier slip and Newtonian heating. Impact of Newtonian heating in flow of power law nanofluid is reported by Hayat et al. [10]. Newtonian heating effects in MHD flow of Jeffrey fluid due to impermeable stretched cylinder is explored by Farooq et al. [11]. Hayat et al.[12] scrutinized the simultaneous impacts of heat source/sink and Newtonian heating in peristaltic flow of micropolar liquid through heterogeneous and homogeneous processes. Thermally radiative stagnation point flow of Powell-Eyring liquid in the presence of Newtonian heating, mixed convection and first order chemical reaction is reported by Hayat et al. [13].

The study of stretched flows of an electrically conducting material has applications in several engineering processes including nuclear reactors, plasma studies, MHD generator, oil exploration and geothermal energy extraction. MHD flow via an artery has receive significant importance in the physiological procedures. Because of such demands the scientists and researchers explored

* Corresponding author.
E-mail address: mw_qau88@yahoo.com (M. Waqas).

http://dx.doi.org/10.1016/j.rinp.2016.10.001
2211-3797/© 2016 Published by Elsevier B.V.

electrically conducting flows under several physical circumstances. For instance Bhattacharyya and Layek [14,15] addressed the MHD boundary layer flow of viscous liquid over a permeable stretched surface with slip conditions and chemical reaction. Haq et al. [16] analyzed convective heat transfer and MHD effects on Casson nanofluid flow over a shrinking sheet. MHD stagnation point flow in presence of chemical reaction and transpiration is reported by Mabood et al. [17]. Sheikh and Abbas [18] explored the influence of thermophoresis in MHD flow over an oscillatory stretched sheet with chemically reactive species. Lin et al. [19] scrutinized unsteady MHD pseudoplastic nanofluid flow over a thin film with internal heat generation. MHD Falkner-Skan flow of nanoliquid is deliberated by Farooq et al. [20]. Shehzad et al. [21] analyzed thermally radiative three-dimensional magneto Jeffrey nanoliquid in presence of internal heat generation. MHD CuO-water nanoliquid in presence of mixed convection is explored by Sheikholeslami et al. [22]. Haq et al. [23] studied MHD squeezed flow of nanofluid over a sensor surface.

Literature survey indicates that less consideration has been given to stretched flows and heat transfer towards radially stretched surface with linear velocity. Even such attempts further narrowed down when stretching surface with nonlinear velocity is considered. Few studies in this direction can be mentioned through Refs. [24, 25, 26, 27]. Further the heat transfer in stretching flow is extensively studied either through imposed surface temperature or heat flux. Heat transfer through Newtonian heating in stretched flow is also less attended. Thus our main motto is to report the characteristics of magnetohydrodynamic (MHD) flow of Jeffrey fluid by a nonlinear radially stretched sheet with Newtonian heating. In addition Joule heating effect is taken into account. Homotopic algorithm [28, 29, 30, 31, 32, 33, 34, 35, 36, 37, 38, 39, 40, 41, 42, 43, 44, 45] is developed to find the expressions of velocity and temperature. Convergence of the developed series solutions is verified. Physical interpretation for the quantities of interest is made.

Formulation

Consider the steady two-dimensional (2D) (r, z) flow of an electrically conducting Jeffrey liquid induced by a radially stretched sheet at $z = 0$ with power law velocity $u_w(r) = ar^n$ where $(a > 0, n > 0)$. A non-uniform magnetic field $B(r) = B_0 r^{n-1/2}$ is applied. Magnetic Reynolds number is chosen small. Induced magnetic and electric fields are neglected. Further heat transfer process is presented in presence of Newtonian heating, Joule heating and heat generation/absorption. Viscous dissipation effects are neglected in heat transfer process. The equations governing the boundary layer flow, heat and mass transfer are:

$$\frac{\partial u}{\partial r} + \frac{u}{r} + \frac{\partial w}{\partial z} = 0, \tag{1}$$

$$u\frac{\partial u}{\partial r} + w\frac{\partial u}{\partial z} = \frac{\nu}{1+\lambda_1}\left(\frac{\partial^2 u}{\partial z^2} + \lambda_2\left(u\frac{\partial^3 u}{\partial r \partial z^2} + w\frac{\partial^3 u}{\partial z^3} + \frac{\partial u}{\partial z}\frac{\partial^2 u}{\partial r \partial z} + \frac{\partial w}{\partial z}\frac{\partial^2 u}{\partial z^2}\right)\right) - \frac{\sigma B^2(r)}{\rho}u, \tag{2}$$

$$u\frac{\partial T}{\partial r} + w\frac{\partial T}{\partial z} = \frac{k}{\rho c_p}\left(\frac{\partial^2 T}{\partial z^2}\right) + \frac{\sigma B^2(r)}{\rho c_p}u^2 + \frac{Q(r)}{\rho c_p}(T - T_\infty), \tag{3}$$

with the boundary conditions

$$\begin{aligned} &u = u_w(r) = ar^n,\ w = 0,\ \tfrac{\partial T}{\partial z} = -h_s T \text{ at } z = 0,\\ &u \to 0,\ T \to T_\infty \text{ as } z \to \infty. \end{aligned} \tag{4}$$

In the aforementioned expressions u and w are the velocity components along radial r and axial z directions respectively, λ_1 the ratio of relaxation to retardation times, λ_2 the retardation time, $Q(r) = Q_0 r^{n-1}$ the non-uniform heat generation/absorption, Q_0 the constant heat generation/absorption, $\nu = \mu/\rho$ the kinematic viscosity, μ the dynamic viscosity of fluid, ρ the fluid density, c_p the specific heat, T the fluid temperature, T_∞ the ambient fluid temperature, n the power index, $u_w(r)$ the stretching velocity, σ the electrical conductivity, k the thermal conductivity, a the dimensional constant with dimension $1/T$ and h_s the convective heat transfer coefficient.

Employing the following transformations [24]:

$$\begin{aligned} &u = ar^n f'(\eta),\ w = -ar^{(n-1)/2}\sqrt{\tfrac{\nu}{a}}\left(\tfrac{n+3}{2}f(\eta) + \tfrac{n-1}{2}\eta f'(\eta)\right),\\ &\eta = \sqrt{\tfrac{a}{\nu}}r^{(n-1)/2}z,\ \theta(\eta) = \tfrac{T-T_\infty}{T_\infty}, \end{aligned} \tag{5}$$

the continuity equation (1) is identically satisfied and Eqs. (2)–(4) are reduced as follows:

$$\begin{aligned} &f''' + \beta\left(\left(\tfrac{3n-5}{2}\right)f'f''' - \left(\tfrac{n+3}{2}\right)ff^{\text{iv}} + \left(\tfrac{3n-1}{2}\right)f''^2\right)\\ &+(1+\lambda_1)\left(\left(\tfrac{n+3}{2}\right)ff'' - nf'^2 - Ha^2 f'\right) = 0, \end{aligned} \tag{6}$$

$$\theta'' + \Pr\left(\left(\frac{n+3}{2}\right)f\theta' + Ha^2 Ec f'^2\right) + S\Pr\theta = 0, \tag{7}$$

$$\begin{aligned} &f'(0) = 1,\ f(0) = 0,\ \theta'(0) = -\gamma(1 + \theta(0)),\\ &f'(\eta) \to 0,\ \theta(\eta) \to 0 \text{ as } \eta \to \infty, \end{aligned} \tag{8}$$

where prime represents the differentiation with respect to η, Pr the Prandtl number, β the Deborah number, parameter S shows heat generation for $(S > 0)$ and absorption when $(S < 0)$, γ the conjugate parameter of Newtonian heating, Ha the Hartman number and Ec the Eckert number. These parameters are defined as follows:

$$\begin{aligned} &\beta = \lambda_2 ar^{n-1},\ \Pr = \tfrac{\nu}{\alpha},\ \alpha = \tfrac{k}{\rho c_p},\ S = \tfrac{Q(r)}{\rho c_p ar^{n-1}},\ \gamma = \tfrac{h_s}{\sqrt{\frac{a}{\nu}}r^{(n-1)/2}},\\ &Ec = \tfrac{u_w^2}{T_\infty c_p},\ Ha^2 = \tfrac{\sigma B^2(r)}{\rho ar^{n-1}}. \end{aligned} \tag{9}$$

Skin friction coefficient and local Nusselt number can be presented into the following forms:

$$C_f = \left(\frac{2\tau_w}{\rho u_w^2}\right)_{z=0}, \tag{10}$$

$$Nu_r = \left(\frac{rq_w}{k(T - T_\infty)}\right)_{z=0}, \tag{11}$$

in which surface shear stress τ_w and surface heat flux q_w are

$$\begin{aligned} &\tau_w = \tfrac{\mu}{1+\lambda_1}\left[\tfrac{\partial u}{\partial z} + \lambda_2\left(u\tfrac{\partial^2 u}{\partial r \partial z} + w\tfrac{\partial^2 u}{\partial z^2}\right)\right]_{z=0},\\ &q_w = -k\left(\tfrac{\partial T}{\partial z}\right)_{z=0}. \end{aligned} \tag{12}$$

Substituting Eq. (12) in Eq. (10) and (11) the skin friction coefficient and local Nusselt number in dimensionless forms are

$$Re_r^{1/2}C_f = \frac{2}{1+\lambda_1}\left(f''(0) + \beta\left\{\frac{3n-1}{2}f'(0)f''(0) - \left(\frac{n+3}{2}\right)f(0)f'''(0)\right\}\right), \tag{13}$$

$$Nu_r Re_r^{-1/2} = \gamma\left(1 + \frac{1}{\theta(0)}\right), \tag{14}$$

where $Re_r = ar^{n+1}/\nu$ is the local Reynolds number.

Homotopy solution

In order to develop solutions we employ the homotopic technique suggested by Liao [28]. The HAM is preferred due to the following facts. (i) The HAM does not require any small/large parameters in the problem. (ii) It gives us a way to verify the convergence of the developed series solutions. (iii) It is useful in providing incredible flexibility in the developing equation type of linear functions of solutions.

In perspective of the boundary conditions given in Eq. (8), we select the set of initial guesses in the forms:

$$f_0(\eta) = (1 - e^{-\eta}),\ \theta_0(\eta) = \left(\frac{\gamma}{1-\gamma}\right)\exp(-\eta), \tag{15}$$

and linear operators satisfying the properties

$$\mathcal{L}_f = f''' - f',\ \mathcal{L}_\theta = \theta'' - \theta, \tag{16}$$

$$\mathcal{L}_f(C_1 + C_2 e^{\eta} + C_3 e^{-\eta}) = 0,\ \mathcal{L}_g(C_4 e^{\eta} + C_5 e^{-\eta}) = 0, \tag{17}$$

where C_i $(i = 1-5)$ indicate the arbitrary constants.

Zeroth-order deformation problems

The corresponding problems at the zeroth order are presented in the following forms:

$$(1-q)\mathcal{L}_f\left[\hat{f}(\eta;q) - f_0(\eta)\right] = q\hbar_f \mathcal{N}_f\left[\hat{f}(\eta;q)\right], \tag{18}$$

$$(1-q)\mathcal{L}_\theta\left[\hat{\theta}(\eta;q) - \theta_0(\eta)\right] = q\hbar_\theta \mathcal{N}_\theta\left[\hat{f}(\eta;q), \hat{\theta}(\eta,q)\right], \tag{19}$$

$$\begin{aligned}&\hat{f}(0;q) = 0,\ \hat{f}'(0;q) = 1,\ \hat{\theta}'(0,q) = -\gamma(1+\theta(0)),\\ &\hat{\theta}(\infty,q) = 0,\ \hat{f}'(\infty;q) = 0.\end{aligned} \tag{20}$$

$$\begin{aligned}\mathcal{N}_f[\hat{f}(\eta,q)] = \frac{\partial^3 \hat{f}(\eta,q)}{\partial\eta^3} &+ \beta\begin{pmatrix} \left(\frac{3n-1}{2}\right)\left(\frac{\partial^2\hat{f}(\eta,q)}{\partial\eta^2}\right)^2 + \left(\frac{3n-5}{2}\right)\frac{\partial\hat{f}(\eta,q)}{\partial\eta}\frac{\partial^3\hat{f}(\eta,q)}{\partial\eta^3} \\ -\left(\frac{n+3}{2}\right)\hat{f}(\eta;q)\frac{\partial^4\hat{f}(\eta,q)}{\partial\eta^4}\end{pmatrix}\\ &+ (1+\lambda_1)\begin{pmatrix}\left(\frac{n+3}{2}\right)\hat{f}(\eta,q)\frac{\partial^2\hat{f}(\eta,q)}{\partial\eta^2} \\ -n\left(\frac{\partial\hat{f}(\eta,q)}{\partial\eta}\right)^2 - Ha^2\frac{\partial\hat{f}(\eta,q)}{\partial\eta}\end{pmatrix},\end{aligned} \tag{21}$$

$$\mathcal{N}_\theta[\hat{f}(\eta,q),\hat{\theta}(\eta,q)] = \frac{\partial^2\hat{\theta}(\eta,q)}{\partial\eta^2} + \Pr\begin{pmatrix}\frac{n+3}{2}\hat{f}(\eta,q)\frac{\partial\hat{\theta}(\eta,q)}{\partial\eta} + Ha^2 Ec\left(\frac{\partial\hat{f}(\eta,q)}{\partial\eta}\right)^2 \\ +S\hat{\theta}(\eta,q)\end{pmatrix}. \tag{22}$$

Here q is an embedding parameter, $\hbar_f$ and $\hbar_\theta$ the non-zero auxiliary parameters and $\mathcal{N}_f$ and $\mathcal{N}_\theta$ indicate the nonlinear operators.

mth-order deformation problems

$$\mathcal{L}_f\left[f_m(\eta) - \chi_m f_{m-1}(\eta)\right] = \hbar_f R_m^f(\eta), \tag{23}$$

$$\mathcal{L}_\theta\left[\theta_m(\eta) - \chi_m \theta_{m-1}(\eta)\right] = \hbar_\theta R_m^\theta(\eta), \tag{24}$$

$$\begin{aligned}&f_m'(0) = 0,\ f_m(0) = 0,\ \theta_m'(0) + \gamma\theta_m(0) = 0,\\ &f_m'(\infty) = 0,\ \theta_m(\infty) = 0,\end{aligned} \tag{25}$$

$$\begin{aligned}R_m^f(\eta) &= f'''_{m-1} + \beta\sum_{k=0}^{m-1}\begin{pmatrix}\left(\frac{3n-1}{2}\right)f'_{m-1-k}f'_k + \left(\frac{3n-5}{2}\right)f'_{m-1-k}f'''_k \\ -\left(\frac{n+3}{2}\right)f_{m-1-k}f^{\mathrm{iv}}_k\end{pmatrix}\\ &+(1+\lambda_1)\sum_{k=0}^{m-1}\left(\left(\frac{n+3}{2}\right)f'_{m-1-k}f''_k - nf'_{m-1-k}f'_k\right)\\ &-(1+\lambda_1)Ha^2\sum_{k=0}^{m-1}f'_{m-1-k},\end{aligned} \tag{26}$$

$$\begin{aligned}R_m^\theta(\eta) = \theta''_{m-1} &+ \Pr\sum_{k=0}^{m-1}\left(\frac{n+3}{2}f_{m-1-k}\theta'_k + Ha^2 Ecf'_{m-1-k}f'_k\right)\\ &+ S\Pr\theta_{m-1}\end{aligned} \tag{27}$$

$$\chi_m = \begin{bmatrix}0,\ m \leqslant 1,\\ 1,\ m > 1\end{bmatrix} \tag{28}$$

The general solutions (f_m, θ_m) consisting of special solutions (f_m^*, θ_m^*) are

$$f_m(\eta) = f_m^*(\eta) + C_1 + C_2 e^{\eta} + C_3 e^{-\eta}, \tag{29}$$

$$\theta_m(\eta) = \theta_m^*(\eta) + C_4 e^{\eta} + C_5 e^{-\eta}, \tag{30}$$

in which the values of $C_i (i = 1-5)$ are

$$\begin{aligned}&C_2 = C_4 = 0,\ C_3 = \left(\frac{\partial f_m^*(\eta)}{\partial\eta}\right)_{\eta=0},\ C_1 = -C_3 - f_m^*(0),\\ &C_5 = \frac{\left(\frac{\partial\theta_m^*(\eta)}{\partial\eta} + \gamma\theta_m^*(\eta)\right)_{\eta=0}}{1-\gamma}.\end{aligned} \tag{31}$$

Convergence

The developed series solutions consist of the non-zero auxiliary parameters $\hbar_f$ and $\hbar_\theta$. These parameters are important in controlling and adjusting the convergence of the HAM solutions. For this purpose we have plotted the $\hbar$-curves of the functions $f''(0)$ and $\theta'(0)$ for the admissible values of $\hbar_f$ and $\hbar_\theta$ at 15th-order of approximations in Fig. 1. Admissible values of $\hbar_f$ and $\hbar_\theta$ are noted $-1.35 \leqslant \hbar_f \leqslant -0.11$ and $-1.51 \leqslant \hbar_\theta \leqslant -0.12$.

Discussion

In order to scrutinize the impacts of several sundry variables on velocity $f'(\eta)$ and temperature $\theta(\eta)$, the Figs. 2–11 are portrayed. Effect of Hartman number Ha on the velocity distribution is plotted in Fig. 2. Velocity and momentum boundary layer thickness are reduced for larger Ha. Physically Lorentz force enhances for larger Ha which is a resistive force and thus the velocity of material reduces. Fig. 3 describes the impact of Deborah number β on the velocity distribution. It is noted that fluid velocity and momentum boundary layer thickness show increasing behavior for larger β. Since Deborah number is directly proportional to retardation time (λ_2) and fluid velocity must increase for larger retardation time.

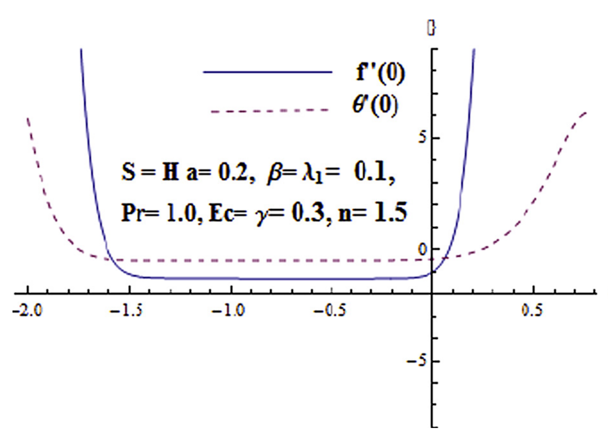

Fig. 1. $\hbar$-curves for $f(\eta)$ and $\theta(\eta)$.

Behavior of λ_1 on the velocity distribution is portrayed in Fig. 4. Velocity shows decreasing behavior for larger λ_1. Physically λ_1 is ratio of relaxation to the retardation times so with an increase in λ_1 the relaxation time also enhances. Consequently drag forces increase and as a result more resistance to the motion of the fluid is provided. That is why the velocity distribution decreases. Fig. 5 depicts the influence of power index n on velocity distribution. Velocity distribution reduces for larger n. Characteristics of Prandtl number on the thermal boundary layer for fixed values of other parameters are depicted in Fig. 6. It depicts that the effect of Pr on the thermal boundary is very prominent. Larger Pr decreases the thermal boundary layer thickness which results in argumentation of heat transfer and consequently temperature of the fluid decreases. Fig. 7 is presented to describe the behavior of heat generation/absorption parameter S on the temperature. Here temperature distribution enhances for larger S. However opposite behavior is examined in case of heat absorption process. Physically more heat is generated in the process of heat generation. Fig. 8 is portrayed to see the influence of power index n on temperature distribution. Temperature distribution reduces for higher values

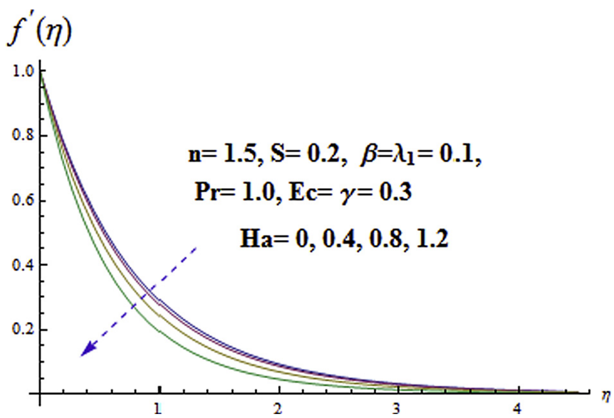

Fig. 2. f' via Ha.

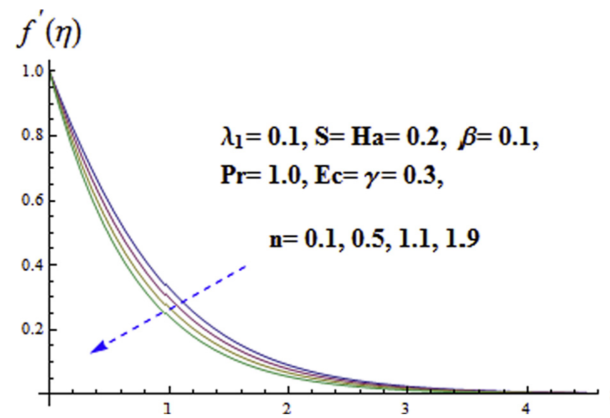

Fig. 5. f' via n.

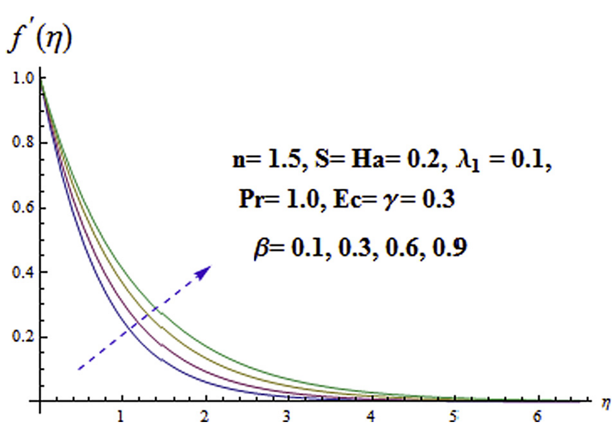

Fig. 3. f' via β.

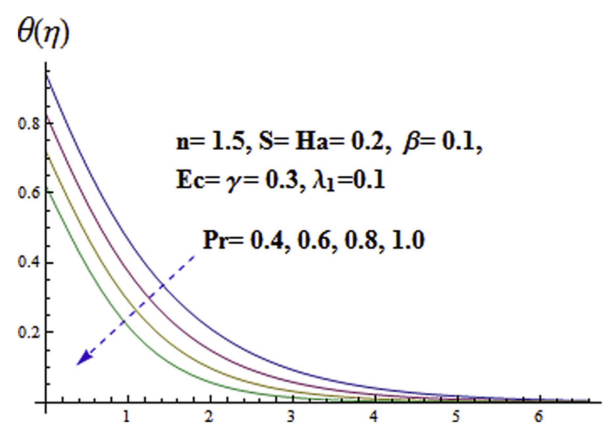

Fig. 6. θ via Pr.

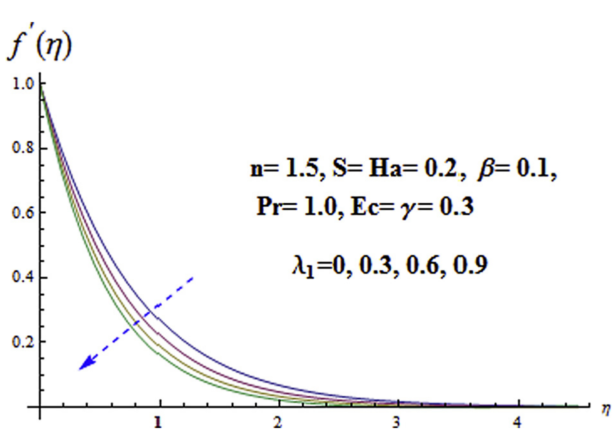

Fig. 4. f' via λ_1.

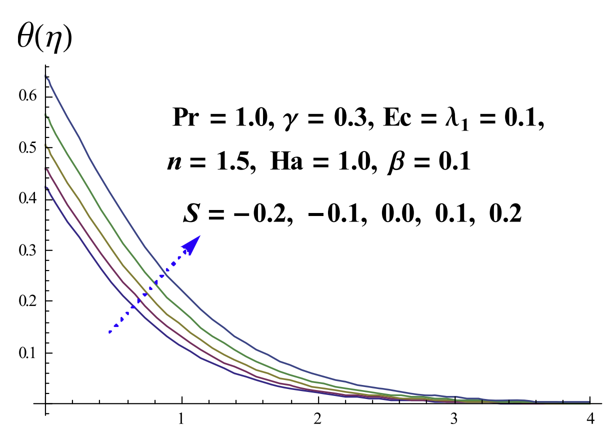

Fig. 7. θ via S.

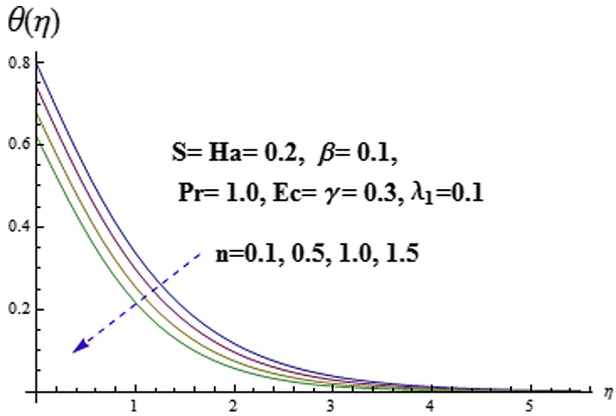

Fig. 8. θ via n.

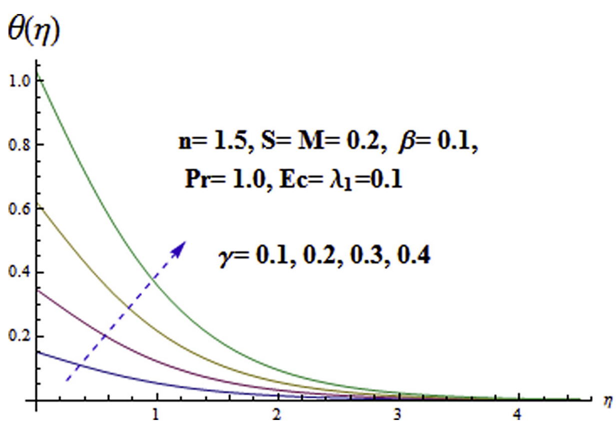

Fig. 9. θ via γ.

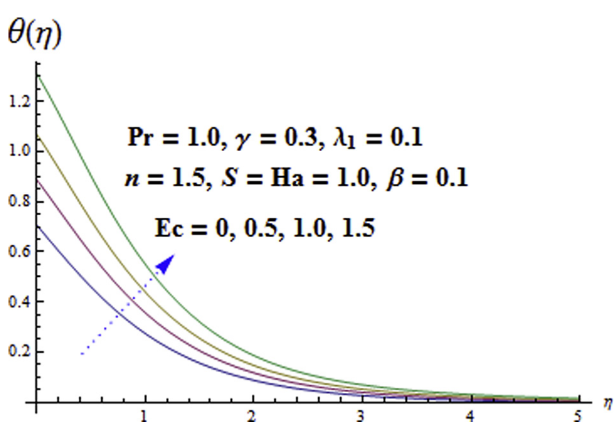

Fig. 10. θ via Ec.

of n but thermal boundary layer enhances. Impact of conjugate parameter γ on temperature $\theta(\eta)$ is shown in Fig. 9. Clearly larger conjugate parameter enhance the heat transfer rate which boosts temperature of material and thermal boundary layer thickness. Fig. 10 delineates the effect of Eckert number Ec on temperature. Physically for larger Ec the material particles are more active due to large amount of energy storage. Hence both the temperature and thermal boundary layer thickness are enhanced. Features of Hartman number Ha on the temperature distribution is portrayed in Fig. 11. It is found that the temperature and thermal boundary

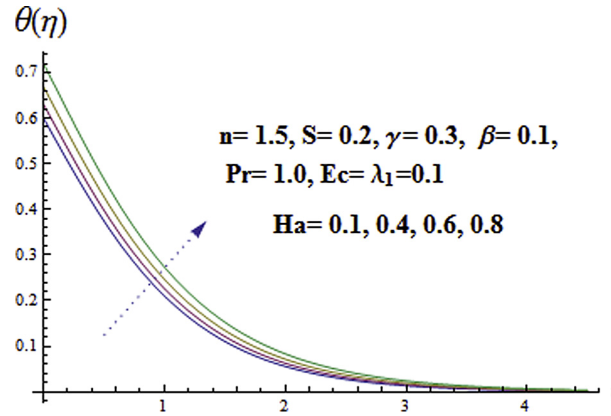

Fig. 11. θ via Ha.

Table 1
Convergence of homotopy solutions for different order of approximations when $\beta = \lambda_1 = 0.1,\ S = Ha = 0.2,\ \gamma = Ec = 0.3,\ \Pr = 1.0,\ n = 1.5$ and $\hbar_f = \hbar_\theta = -0.5$.

Order of approximations	$-f''(0)$	$-\theta'(0)$
1	1.12160	0.44148
6	1.29413	0.47761
11	1.30834	0.48918
16	1.30952	0.49224
21	1.30958	0.49282
26	1.30958	0.49285
31	1.30958	0.49285
45	1.30958	0.49285

Table 2
Numerical values of skin friction coefficient $C_f Re_r^{1/2}$ for various values of $\beta,\ \lambda_1$, Ha and n when $S = 0.2,\ Pr = 1.0,\ \gamma = 0.3$ and $Ec = 0.3$.

β	λ_1	Ha	n	$C_f Re_r^{1/2}$
0.0	0.1	0.2	1.5	−1.2862
0.02				−1.3094
0.04				−1.3323
0.1	0.0			−1.4670
	0.3			−1.2872
	0.6			−1.1607
	0.1	0.0		−1.3834
		0.3		−1.4180
		0.3		−1.5175
		0.2	0.0	−0.7733
			0.6	−1.0396
			1.2	−1.2821

Table 3
Numerical values of local Nusselt number $Nu_r Re_r^{-\frac{1}{2}}$ for various values of Ha, γ, S, Pr and Ec when $\beta = 0.1, \lambda_1 = 0.1$, and $n = 1.5$.

S	Ha	γ	Pr	Ec	$Nu_r Re_r^{-\frac{1}{2}}$
0.0	0.2	0.3	1.0	0.3	0.8955
0.1					0.8340
0.3					0.6923
0.2	0.1				0.7737
	0.3				0.7551
	0.4				0.7398
	0.2	0.2			0.7452
		0.4			0.7521
		0.5			0.7535
		0.3	0.8		0.6461
			0.9		0.7084
			1.1		0.8225
			1.0	0.1	0.7704
				0.2	0.7684
				0.4	0.7646

layer are enhanced for larger *Ha*. Lorentz force enhances for larger *Ha* and more heat is generated. This leads to an augment in temperature distribution.

Table 1 is displayed to visualize the convergent values of $-f''(0)$ and $-\theta'(0)$ for fixed values of emerging parameters. Clearly the velocity and temperature equations converge at 26th and 31th order of approximations respectively. It is noted that the values of velocity are larger when compared with temperature. Impacts of β, Ha, λ_1 and n on skin friction coefficient are shown in Table 2. It is found that skin friction coefficient enhances for larger β, Ha and n while it reduces via λ_1. Table 3 portrays the influences of S, Ha, γ, Pr and Ec on local Nusselt number. Tabulated values clearly indicate that the values of Nusselt number are enhanced for higher values of γ and Pr further it is decrease via larger *S, Ha* and *Ec*.

Conclusions

The present study explores the hydromagnetic flow of Jeffrey fluid in the presence of Joule and Newtonian heatings by a nonlinear stretching sheet. The main results are listed below:

- Impacts of Ha, λ_1 and n on f' are equivalent in a qualitative manner.
- Higher values of Deborah number β result in the enhancement of the velocity and momentum boundary layer thickness.
- There are opposite effects of Hartman number *Ha* on the velocity and temperature.
- Behaviors of Prandtl number *Pr* and power index n on temperature are similar.
- Velocity and temperature distributions are reduced for higher values of power index n.
- Skin friction coefficient enhances for larger β, Ha and n.
- Local Nusselt number is an increasing function of γ and *Pr*.

References

[1] Hayat T, Waqas M, Shehzad SA, Alsaedi A. MHD stagnation point flow of Jeffrey fluid by a radially stretching surface with viscous dissipation and Joule heating. J. Hydrol. Hydromech. 2015;63:311–7.
[2] Farooq M, Alsaedi A, Hayat T. Note on characteristics of homogeneous-heterogeneous reaction in flow of Jeffrey fluid. Appl. Math. Mech. 2015;36:1319–28.
[3] Tripathi D, Ali N, Hayat T, Chaube MK, Hendi AA. Peristaltic flow of MHD Jeffrey fluid through a finite length cylindrical tube. Appl. Math. Mech. Engl. Edit. 2011;32:1148–60.
[4] Abbasi FM, Shehzad SA, Hayat T, Alsaedi A, Obid MA. Influence of heat and mass flux conditions in hydromagnetic flow of Jeffrey nanofluid. AIP Adv. 2015;5:037111.
[5] Shehzad SA, Alsaadi FE, Monaquel SJ, Hayat T. Soret and Dufour effects on the stagnation point flow of Jeffrey fluid with convective boundary condition. Eur. Phys. J. Plus 2013;128:56.
[6] Merkin JH. Natural convection boundary layer flow on a vertical surface with Newtonian heating. Int. J. Heat Fluid Flow 1994;15:392–8.
[7] Salleh MZ, Nazar R, Pop I. Boundary layer flow and heat transfer over a stretching sheet with Newtonian heating. J. Taiwan Inst. Chem. Eng. 2010;41:651–5.
[8] Hayat T, Iqbal Z, Mustafa M. Flow of a second grade fluid over a stretching surface with Newtonian heating. J. Mech. 2012;28:209–16.
[9] Makinde OD. and heat transfer toward a flat plate with Navier slip and Newtonian heating. Braz. J. Chem. Eng. 2012;29:159–66.
[10] Hayat T, Hussain M, Alsaedi A, Shehzad SA, Chen GQ. Flow of power-law nanofluid over a stretching surface with Newtonian heating. J. Appl. Fluid Mech. 2015;8:273–80.
[11] Farooq M, Gull N, Alsaedi A, Hayat T. MHD flow of a Jeffrey fluid with Newtonian heating. J. Mech. 2015;31:319–29.
[12] Hayat T, Farooq S, Ahmad B, Alsaedi A. Homogeneous-heterogeneous reactions and heat source/sink effects in MHD peristaltic flow of micropolar fluid with Newtonian heating in a curved channel. J. Mol. Liq. 2016;223:469–88.
[13] Hayat T, Waqas M, Shehzad SA, Alsaedi A. Mixed convection stagnation-point flow of Powell-Eyring fluid with Newtonian heating, thermal radiation and heat generation/absorption. J. Aerospace Eng. 2016. DOI:http://dx.doi.org/10.106/(ASCE)AS.1943-5525.0000674.
[14] Bhattacharyya K, Layek GC. Chemically reactive solute distribution in MHD boundary layer flow over a permeable stretching sheet with suction or blowing. Chem. Eng. Commun. 2010;197:1527–40.
[15] Bhattacharyya K, Layek GC. Slip effects on diffusion of chemically reactive species in boundary layer flow due to a vertical stretching sheet with suction or blowing. Chem. Eng. Commun. 2011;198:1354–65.
[16] Haq RU, Nadeem S, Khan ZH, Gideon OT. Convective heat transfer and MHD effects on Casson nanofluid flow over a shrinking sheet. Cent. Eur. J. Phys. 2014;12:862–71.
[17] Mabood F, Khan WA, Ismail AIMd. MHD stagnation point flow and heat transfer impinging on stretching sheet with chemical reaction and transpiration. Chem. Eng. J. 2015;273:430–7.
[18] Sheikh M, Abbas Z. Effects of thermophoresis and heat generation/absorption on MHD flow due to an oscillatory stretching sheet with chemically reactive species. J. Magn. Magn. Mater. 2015;396:204–13.
[19] Lin Y, Zheng L, Zhang X, Ma L, Chen G. MHD pseudoplastic nanofluid unsteady flow and heat transfer in a finite thin film over stretching surface with internal heat generation. Int. J. Heat Mass Transfer 2015;84:903–11.
[20] Farooq U, Zhao YL, Hayat T, Alsaedi A. Application of the HAM-based Mathematica package BVPh 2.0 on MHD Falkner-Skan flow of nanofluid. Comput. Fluids 2015;11:69–75.
[21] Shehzad SA, Abdullah Z, Alsaedi A, Abbaasi FM, Hayat T. Thermally radiative three-dimensional flow of Jeffrey nanofluid with internal heat generation and magnetic field. J. Magn. Magn. Mater. 2016;397:108–14.
[22] Sheikholeslami M, Bandpy MG, Ellahi R, Zeeshan A. Simulation of MHD CuO-water nanofluid flow and convective heat transfer considering Lorentz forces. J. Magn. Magn. Mater. 2014;369:69–80.
[23] Haq RU, Nadeem S, Khan ZH, Noor NFM. MHD squeezed flow of water functionalized metallic nanoparticles over a sensor surface. Phys. E 2015;73:45–53.
[24] Mustafa M, Khan JA, Hayat T, Alsaedi A. Analytical and numerical solutions for axisymmetric flow of nanofluid due to non-linearly stretching sheet. Int. J. Nonlinear Mech. 2015;71:22–9.
[25] Awais M, Hayat T, Nawaz M, Alsaedi A, heating Newtonian. thermal-diffusion and diffusion-thermo effects in an axisymmetric flow of a Jeffrey fluid over a stretching surface. Braz. J. Chem. Eng. 2015;32. DOI:10.1590/0104-6632.20150322s0000191.
[26] Ahmed J, Shahzad A, Khan M, Ali R. A note on convective heat transfer of an MHD Jeffrey fluid over a stretching sheet. AIP Adv. 2015;5:117117.
[27] Ahmed J, Mahmood T, Iqbal Z, Shahzad A, Ali R. Axisymmetric flow and heat transfer over an unsteady stretching sheet in power law fluid. J. Mol. Liq. 2016;221:386–93.
[28] Liao SJ. Beyond Perturbation: Introduction to Homotopy Analysis Method. CRC Press, Boca Raton: Chapman and Hall; 2003.
[29] Shehzad A, Ali R, Khan M. On the exact solution for axisymmetric flow and heat transfer over a nonlinear radially stretching sheet. Chin. Phys. Lett. 2012;29:084705.
[30] Han S, Zheng L, Li C, Zhang X. Coupled flow and heat transfer in viscoelastic fluid with Cattaneo-Christov heat flux model. Appl. Math. Lett. 2014;38:87–93.
[31] Sheikholeslami M, Hatami M, Ganji DD. Micropolar fluid flow and heat transfer in a permeable channel using analytical method. J. Mol. Liq. 2014;194:30–6.
[32] Zheng L, Zhang C, Zhang X, Zhang J. Flow and radiation heat transfer of a nanofluid over a stretching sheet with velocity slip and temperature jump in porous medium. J. Franklin Inst. 2013;350:990–1007.
[33] Sheikholeslami M, Ellahi R, Ashorynejad HR, Domairry G, Hayat T. Effect of heat transfer in flow of nanofluids over a permeable stretching wall in a porous medium. J. Comput. Theor. Nanosci. 2014;11:486–96.
[34] Turkyilmazoglu M. An effective approach for evaluation of the optimal convergence control parameter in the homotopy analysis method. Filomat 2016;30:1633–50.
[35] Ali R, Shahzad A, Khan M, Ayub M. Analytic and numerical solutions for axisymmetric flow with partial slip. Eng. Comput. 2016;32:149–54.
[36] Hayat T, Hussain Z, Muhammad T, Alsaedi A. Effects of homogeneous and heterogeneous reactions in flow of nanofluids over a nonlinear stretching surface with variable surface thickness. J. Mol. Liq. 2016;221:1121–7.
[37] Waqas M, Hayat T, Farooq M, Shehzad SA, Alsaedi A. Cattaneo-Christov heat flux model for flow of variable thermal conductivity generalized Burgers fluid. J. Mol. Liq. 2016;220:642–8.
[38] Khan M, Khan WA. Three-dimensional flow and heat transfer to burgers fluid using Cattaneo-Christov heat flux model. J. Mol. Liq. 2016;221:651–7.
[39] Waqas M, Khan MI, Farooq M, Alsaedi A, Hayat T, Yasmeen T. Magnetohydrodynamic (MHD) mixed convection flow of micropolar liquid due to nonlinear stretched sheet with convective condition. Int. J. Heat Mass Transfer 2016;102:766–72.
[40] Shehzad SA, Waqas M, Alsaedi A, Hayat T. Flow and heat transfer over an unsteady stretching sheet in a micropolar fluid with convective boundary condition. J. Appl. Fluid Mech. 2016;9:1437–45.
[41] Hayat T, Waqas M, Shehzad SA, Alsaedi A. A model of solar radiation and Joule heating in magnetohydrodynamic (MHD) convective flow of thixotropic nanofluid. J. Mol. Liq. 2016;215:704–10.
[42] Khan WA, Khan M, Alshomrani AS. Impact of chemical processes on 3D Burgers fluid utilizing Cattaneo-Christov double-diffusion: applications of non-Fourier's heat and non-Fick's mass flux models. J. Mol. Liq. 2016. DOI: 10.1016/j.molliq.2016.09.02.

[43] Farooq M, Khan MI, Waqas M, Hayat T, Alsaedi A, Khan MI. MHD stagnation point flow of viscoelastic nanofluid with non-linear radiation effects. J. Mol. Liq. 2016;221:1097–103.
[44] Hayat T, Bashir G, Waqas M, Alsaedi A. MHD 2D flow of Williamson nanofluid over a nonlinear variable thicked surface with melting heat transfer. J. Mol. Liq. 2016. DOI: 10.1016/j.molliq.2016.08.10.
[45] Hayat T, Khan MI, Waqas M, Alsaedi A, Yasmeen T. Diffusion of chemically reactive species in third grade flow over an exponentially stretching sheet considering magnetic field effects. Chin. J. Chem. Eng. 2016. DOI: 10.1016/j.cjche.2016.06.00.